Int. J. Electrochem. Sci., 16 **(2021)** Article ID: 210451, doi: 10.20964/2021.04.16

International Journal of
ELECTROCHEMICAL
SCIENCE
www.electrochemsci.org

An Electrochemical Sensor Based on Bimetallic PtPd Nanoparticles for the Determination of Bisphenol A

Zhiqiang Zhu[1,*], *Xiangyang Miao*[1], *Danhong Yan*[1]

[1] Suzhou Chien-shiung Institute of Technology, China
[*]E-mail: zhu29@163.com

Received: 2 December 2020 / *Accepted:* 15 January 2021 / *Published:* 28 February 2021

As a chemical compound with low toxicity, bisphenol A (BPA) mimics oestrogen activity, which can induce precocious puberty. Herein, a sensitive electrochemical sensor is constructed for BPA detection based on flower-like bimetallic PtPd nanoparticles, which are synthesized by a microwave-assisted hydrothermal method. After characterization by transmission electron microscopy (TEM), the electrochemical behaviour of BPA on a PtPd nanoparticle-modified glassy carbon electrode (PtPd/GCE) is studied by electrochemical tests, including cyclic voltammetry (CV), electrochemical impedance spectroscopy (EIS) and differential pulse voltammetry (DPV). Under optimal conditions, the electrochemical response of BPA on PtPd/GCE is linear, with BPA concentrations ranging from 0.75 μM to 600 μM and a detection limit of 132 nM. Due to the high sensitivity and stability of this sensor, it is used to detect BPA in both food and beverage containers with satisfactory recoveries and acceptable relative standard deviations.

Keywords: electrochemistry; bimetallic nanoparticle; bisphenol A

1. INTRODUCTION

Bisphenol A (BPA, 2,2-bis(4-hydroxyphenyl) propane) is a worldwide chemical compound that has been extensively used in the packaging of canned food and beverages, milk bottles, water bottles, eyeglass lenses and hundreds of other daily necessities. Unfortunately, BPA is considered an endocrine disrupting chemical (EDC) that may alter hormonal function [1-4]. Further studies have proven that BPA mimics oestrogen activity, which can induce precocious puberty at very low concentrations. Thus, it is very important to develop sensitive analytical methods for the determination of BPA in plastic containers to ensure food safety.

Many novel analytical techniques have been employed to determine BPA in recent years [5-7], such as gas chromatography coupled with mass spectrometry (GC-MS) [8, 9], high-performance liquid chromatography (HPLC) [10], electrochemistry [11, 12] and chemiluminescence (CL) [13]. Among these techniques, electrochemical sensors exhibit superior advantages, namely, their short response time,

high sensitivity, easy operation and low cost; thus, the use of electrochemical sensors are considered an ideal method for BPA detection. With the development of nanotechnology, nanomaterials have been introduced in the construction of electrochemical sensors [14, 15], improving the analytical performance of electrochemical sensors for BPA detection due to their large surface area, excellent conductivity and high catalytic ability. For example, graphene oxide [16, 17], multiwalled carbon nanotubes [18], gold nanoparticles [19, 20], silver nanoparticles [21] and titanium dioxide nanoparticles [22] have been used to construct electrochemical sensors for the determination of bisphenol A.

In this study, bimetallic PtPd nanoparticles are synthetized to electrochemically determine BPA with high sensitivity. Noble metal nanoparticles possess excellent chemical and physical properties and are extensively employed to construct electrochemical sensors for BPA detection. Compared to single noble metal nanoparticles, dual noble metal nanoparticles have been increasingly studied due to the synergistic effect between the two noble metals, which can greatly enhance the analytical performance of electrochemical sensors [23-25]. On the basis of this concept, a sensitive electrochemical sensor is designed for the detection of BPA based on bimetallic PtPd nanoparticles (Scheme 1). The analytical performance of this sensor is evaluated in an ideal buffer and in real samples, proving that the designed sensor is a useful tool for BPA determination.

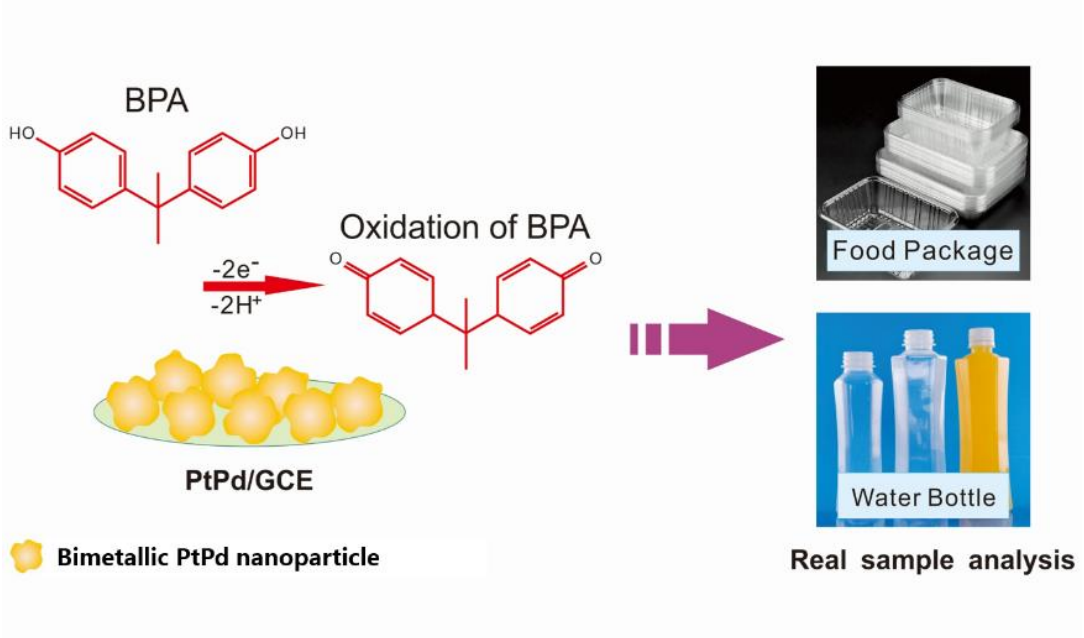

Scheme 1. Schematic illustration showing the determination of BPA with PtPd/GCE.

2. EXPERIMENTAL

2.1. Chemicals and reagents

Potassium platinochloride (K_2PtCl_4), potassium chloropalladite (K_2PdCl_4), sodium dihydrogen phosphate (NaH_2PO_4), disodium hydrogen phosphate (Na2HPO4), N,N-dimethylformamide (DMF), ethanol and potassium iodide (KI) were purchased from Sinopharm Chemical Reagent Co., Ltd. (China). 2,2-Bis(4-hydroxyphenyl) propane (bisphenol A), polyvinylpyrrolidone (PVP), potassium

hexacyanoferrate(II) trihydrate, and potassium ferricyanide(III) were purchased from Sigma-Aldrich Ltd. All aqueous solutions were prepared with twice-deionized water.

2.2. Apparatus

All electrochemical measurements were carried out on a PGSTAT302 Autolab instrument (Metrohm China, Ltd.). A conventional three-electrode system was employed, consisting of a glassy carbon electrode (GCE) as the working electrode, an Ag/AgCl (3 M KCl) electrode as the reference electrode and a platinum wire electrode as the counter electrode. TEM was performed with a Hitachi H-7500 electron microscope (120 kV).

2.3. Synthesis of the bimetallic PtPd nanoparticles

PtPd nanoparticles were synthesized according to published works with some modifications [26, 27]. Briefly, 0.2 g of KI and 0.25 g of PVP were added to 1 mL of twice-deionized water and stirred for 15 min. The above solution was mixed with a 240 μL (100 mM) potassium platinochloride solution, 240 μL (100 mM) potassium chloropalladite solution and 4 mL DMF solution and then magnetically stirred well. The mixture was heated in a microwave reactor at 130 °C for 30 min. Subsequently, the bimetallic PtPd nanoparticles were centrifuged and washed twice at room temperature. Finally, the bimetallic PtPd nanoparticles were dissolved in 1 mL of water and kept at 4 °C. Pt nanoparticles were synthesized by the same method without the addition of potassium chloropalladite.

2.4. Preparation of the modified electrode

Prior to modification, the bimetallic PtPd nanoparticles were diluted to a concentration of 100 μg/mL. All working electrodes were polished with 0.3 μm and 0.05 μm alumina and then sequentially sonicated in ethanol and deionized water. After cleaning, the bimetallic PtPd nanoparticles were added dropwise onto the glassy carbon electrode surface to form a bimetallic PtPd nanoparticle-modified electrode, which was labelled as PtPd/GCE. Electrolyte solutions were deoxygenated with dry nitrogen by bubbling for at least 30 min, and a nitrogen atmosphere was kept over the solution for electrochemical measurements.

2.5. Determination of BPA in real samples

Plastic was cut into small pieces and then washed twice with distilled water. Then, the small plastic pieces and ethanol were added into a conical bottle. The mixture was ultrasonicated for 30 min and kept at 50 °C for 4 hours. After the small plastic pieces were completely dissolved, the solution was transferred to a 100 mL volumetric flask and diluted to a certain concentration.

3. RESULTS AND DISCUSSION

3.1. Characterization of the bimetallic PtPd nanoparticles

TEM was applied to prove the successful synthesis of the bimetallic PtPd nanoparticles. As shown in Fig. 1, the morphology of the PtPd nanoparticles was compared with that of the Pt nanoparticles. The diameter of the PtPd nanoparticles was approximately 16.1±1.4 nm (Fig. 1A), which was smaller than that of the pure Pt nanoparticles (19.0±1.6 nm, Fig. 1B). Moreover, a typical flower-like structure was observed with the bimetallic PtPd nanoparticles, while the Pt nanoparticles had an irregular structure. The uniform nanocrystals indicated the high-yield synthesis of the bimetallic PtPd nanoparticles. The catalytic activity of the bimetallic PtPd nanoparticles was shape-dependent [27]. Compared to the Pt nanoparticles, the shape of the bimetallic PtPd nanoparticles resulted in a larger surface area, suggesting that the bimetallic PtPd nanoparticles had a larger electroactive area than the pure Pt nanoparticles.

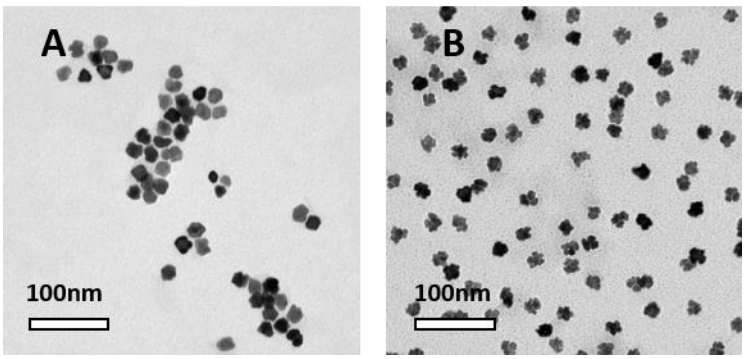

Figure 1. TEM images of the (A) Pt nanoparticles and (B) PtPd nanoparticles.

3.2. Electrochemical behaviour of BPA on PtPd/GCE

The electrochemical properties of PtPd/GCE were investigated by electrochemical tests. As shown in Fig. S1, cyclic voltammetry (CV) curves were recorded in a 0.1 M KCl solution with $K_3[Fe(CN)_6]/K_4[Fe(CN)_6]$ as the redox probe. A pair of redox peaks was observed with a bare GCE. A larger peak current was obtained with PtPd/GCE, which was ascribed to the high conductivity of the bimetallic PtPd nanoparticles [28]. Electrochemical impedance spectroscopy (EIS) was used to further investigate the electrochemical properties of PtPd/GCE, and the results are shown in Fig. 2A. It is well known that the diameter of the semicircle is equal to the charge transfer resistance (R_{et}) at high frequency. The R_{et} values of Pt/GCE and PtPd/GCE were approximately 36.2 Ω and 15.6 Ω, respectively, which were smaller than that with a bare GCE (224.6 Ω), suggesting that the conductivity of the electrode was improved by the functionalization of both Pt and PtPd on the GCE surface.

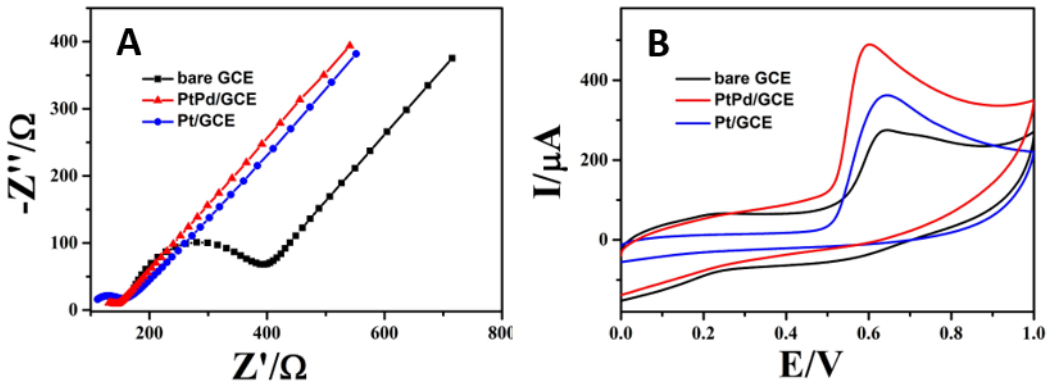

Figure 2. (A) EIS curves of the bare GCE, Pt/GCE and PtPd/GCE in 0.1 mM $[Fe(CN)_6]^{4-}$ and $[Fe(CN)_6]^{3-}$ solutions containing 0.1 M KCl. (B) CV curves of the bare GCE, Pt/GCE and PtPd/GCE in a 0.2 mM PB solution containing 50 μM BPA.

The analytical performance of Pt/GCE and PtPd/GCE was tested by CV. An obvious oxidation peak located at 0.64 V was observed with the bare GCE in the presence of 50 μM BPA. After decorating a GCE with Pt nanoparticles and bimetallic PtPd nanoparticles, the peak currents when Pt/GCE and PtPd/GCE were used showed significant increases. Moreover, the peak potential of PtPd/GCE (0.60 V) shifted negatively compared to that of the bare GCE, proving that the bimetallic PtPd nanoparticles could efficiently improve the electrocatalytic oxidation of BPA and decrease the overpotential of BPA oxidation. It is noted that the bimetallic PtPd nanoparticles had better electrocatalytic ability towards BPA oxidation, providing a higher peak current and more negative potential. All experimental results suggested that PtPd/GCE could be used to determine BPA.

3.3. Effect of pH

The effect of pH on the analytical performance of PtPd/GCE was investigated. As shown in Fig. 3, the oxidation peak of BPA shifted negatively when the pH ranged from 3.5 to 8.0. A linear relationship between the peak potential and pH was obtained, and the linear regression equation was expressed as $E_{pa}(V) = -0.0643pH + 1.017$ (R^2=0.995, Fig. 3B). The slope of -64.3 mV pH^{-1} was near to the theoretical value (-59.2 mV pH^{-1}), indicating that the number of transferred electrons and protons in the electrochemical oxidation of BPA were the same. Furthermore, the largest peak current of BPA was obtained when the pH was 6.0 (Fig. S2). Therefore, pH 6.0 was chosen as the optimal detection condition. The optimal pH was lower than the pKa of BPA (9.73), indicating that non-dissociated BPA was involved in the electrocatalysis process [29].

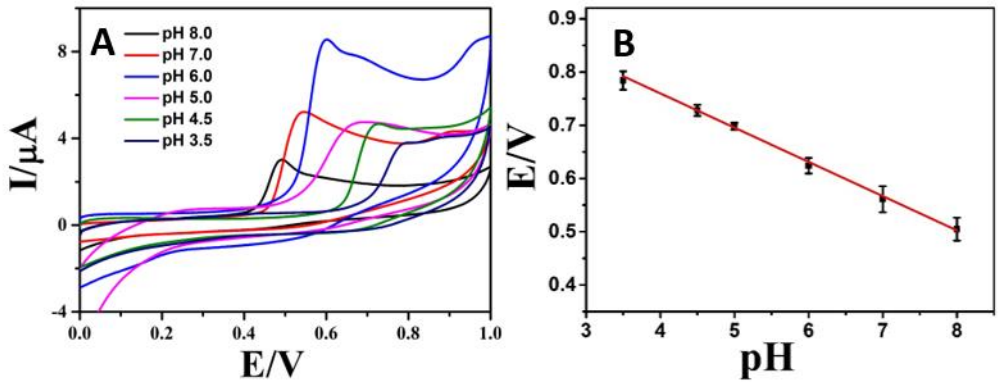

Figure 3. (A) CV curves of 50 μM BPA on PtPd/GCE with the pH ranging from 3.5 to 8.0. (B) Effects of pH on the oxidation peak potential.

3.4. Effect of scan rates

The effect of the scan rate on the oxidation peak current was also studied (Fig. S3, Fig. 4a). The peak current (I_{pa}) increased with scan rates ranging from 10 mV s^{-1} to 300 mV s^{-1}. Clearly, the peak current was linear with the square root of the scan rate ($v^{1/2}$), and the equation, I_{pa} (μA) =0.448$v^{1/2}$ (mV s^{-1})-0.119 (R^2=0.989), indicates that the electrochemical behaviour of BPA on PtPd/GCE was a typical diffusion-controlled process. The oxidation peak potential (E_{pa}) shifted negatively with an increasing scan rate (Fig. 4b). There was a linear relationship between the peak potential and Napierian logarithm of scan rates ($\ln v$). The linear regression equation was $E_{pa}(V) = -0.0364 \ln v$ (mV s^{-1}) + 0.861 (R^2=0.987). For irreversible electrochemical processes, the relationship between E_{pa} and ln ν can be described as $E_{pa}(V) = E^0 + (RT/\alpha nF) \ln(RTk^0/\alpha nF) + (RT/\alpha nF) \ln v$ [30]. According to the above equation, αn was calculated to be 1.15. Generally, α is assumed to be 0.5 in a totally irreversible electrode process, and in this case, n was calculated to be 2.3 (approximately equal to 2). Therefore, two protons and two electrons were involved in the oxidation process of BPA (Scheme 1). This conclusion was in accordance with a previous report; thus, the observed electrochemical redox mechanism was similar to that in the literature [7, 29].

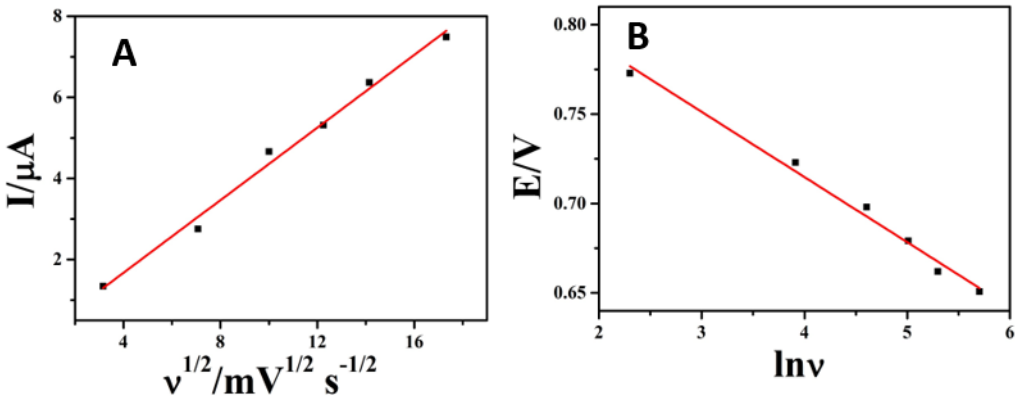

Figure 4. (A) Linear relationship between the peak current (I_{pa}) and the square root of the scan rate (10, 50, 100, 150, 200, 300 mV s^{-1}). (B) Linear relationship between the peak potential (E_{pa}) and the Napierian logarithm of the scan rate.

3.5. Analytical performance of PtPd/GCE for BPA detection

Differential pulse voltammetry (DPV) was applied for the determination of BPA under optimal conditions (Fig. 5). The peak currents of PtPd/GCE increased with the addition of BPA in the range of 0.75-600 μM. A linear relationship was observed between the peak current and BPA concentration with a linear regression equation of $I_{\mathrm{pa}}(\mu\mathrm{A}) = 0.0122C_{\mathrm{BPA}}(\mu\mathrm{M}) + 0.0713$ (R^2=0.994). The limit of detection (LOD) was calculated as 132 nM.

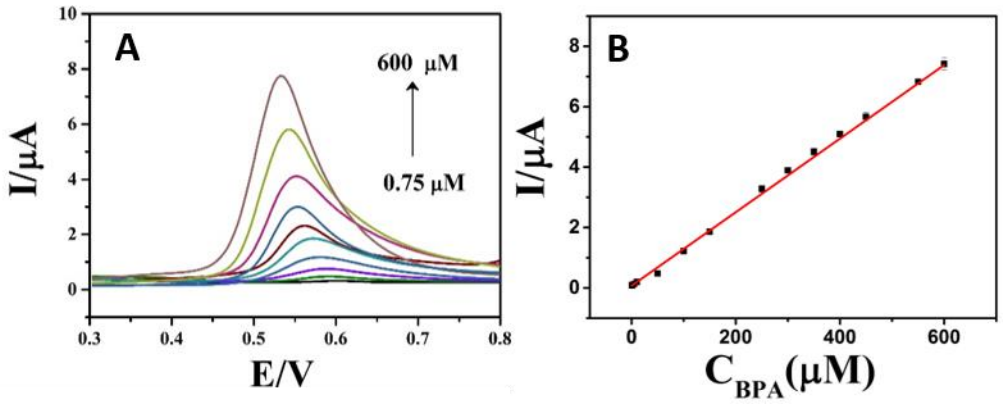

Figure 5. (A) DPV curves of PtPd/GCE for the determination of BPA in the range from 0.75 μM to 600 μM. (B) Corresponding BPA peak current versus BPA concentration.

Table 1. Comparison of the performances of sensors for BPA detection based on their different matrices.

Electrode	Linear range (μmol L^{-1})	Detection limit (μmol L^{-1})	References
Molecularly imprinted polymer-coupled graphitic carbon nitride photoanode	5-100	1.3	12
AuNP/MWCNT/GCE	0.01-0.7	0.004	18
Gr-AgCu/Au electrode	1.31	0.1-100	31
Exfoliated graphite electrode	1.56-50	0.76	32
Thionine-modified carbon paste electrode	0.15-0.45	0.15	33
Magnetic molecularly imprinted nanoparticles on a surfactant-modified magnetic electrode	0.5-150 5-1000	0.17 0.98	34
Copper oxide nanoparticles/ionic liquid/carbon paste electrode	0.2-175	0.1	35
PtPd/GCE	0.75-600	0.132	This work

The performance of PtPd/GCE was comparable to or better than that of previously reported modified electrodes (Table 1). The reproducibility and stability of PtPd/GCE were investigated in the

presence of 50 μM BPA. Five independent PtPd/GCEs were constructed to study their electrochemical responses. The relative standard deviation (RSD) of the corresponding electrochemical responses was 6.1%, suggesting that the designed PtPd/GCE had excellent reproducibility. After storage for two weeks at 4 °C, the peak current of PtPd/GCE for 50 μM BPA detection decreased by 17.4%, proving that the PtPd/GCE showed good long-term stability for the detection of BPA.

3.6. Determination of BPA in real samples

The practical application of PtPd/GCE for the analysis of BPA was investigated in both food and beverage containers by using a standard addition method. Accepted relative standard deviations (RSDs, <5%) and recoveries (~99%) were obtained and are listed in Table 2. These results proved that the prepared bimetallic PtPd nanoparticles were a potential nanomaterial that could be used to construct electrochemical sensors for BPA detection in buffer and real samples.

Table 2. Analytical performance of this sensor for BPA detection in plastic samples (n=3).

Sample	Detected (μM)	Added (μM)	Found (μM)	RSD (%)	Recovery (%)
1[a]	1.63	4.00	5.58	3.74	98.7
2[b]	0.95	4.00	4.93	4.49	99.5

[a] Extract from plastic food packaging materials
[b] Extract from mineral water bottle

4. CONCLUSIONS

In summary, flower-like bimetallic PtPd nanoparticles with high electrocatalytic activity were successfully fabricated via a microwave-assisted synthesis method. The prepared PtPd/GCE exhibited excellent electrocatalytic ability towards BPA oxidation. Under optimal conditions, the electrochemical sensor exhibited a wide linear range (0.75 μM-600 μM), low detection limit (132 nM) and high stability. A real sample analysis further proved that the designed bimetallic PtPd nanoparticles were a promising candidate for constructing electrochemical sensors to detect target molecules.

ACKNOWLEDGEMENTS
This work was supported by the Natural Science Fund for Colleges and Universities in Jiangsu Province (No. 19KJB310017) and the Science and Technology Programme of Taicang (No. TC2018JC03).

References

1. K. J. Groh, T. Backhaus, B. Carneyalmroth, B. Geueke, P. A. Inostroza, A. Lennquist, H. A. Leslie, M. V. Maffini, D. Slunge, L. Trasande, A. Warhurst, J. Muncke, *Sci. Total Environ.*, 651 (2019) 3253.
2. H. M. Yan, M. Takamoto, K. Sugane, *Environ. Health. Perspect.*, 116 (2008) 514.
3. W. Dekant, W. Volkel, *Toxicol. Appl. Pharmacol.*, 228 (2008) 114.

4. W. Volkel, M. Kiranoglu, H. Fromme, *Toxicol. Lett.*, 179 (2008) 155.
5. A. Careghini, A. F. Mastorgio, S. Saponaro, E. Sezenna, *Environ. Sci. Pollut. Res.*, 22 (2015) 5711-5741.
6. Dhanjai, A. Sinha A, L. X. Wu, X. B. Lu, J. P. Chen, R. Jain, *Anal. Chim. Acta.*, 998 (2018) 1.
7. L. A. Gugoasa, *J. Electrochem. Soc.*, 167 (2020) 037506.
8. A. Jurek, E. Leitner *Food Addit. Contam. A*, 34 (2017) 1225-1238.
9. N. Dreolin, M. Aznar, S. Moret, C. Nerin, *Food Chem.*, 274 (2019) 246.
10. M. K. Manoj, R. Ramakrishnan, S. Babjee, R. Nasim, *Am. J. Orthod. Dentofacial. Orthop.*, 154 (2018) 803.
11. V. M. Ekomo, C. Branger, R. Bikanga, A. Florea, G. Istamboulie, C. Calasblanchard, T. Noguer, A. Sarbu, H. Brisset, *Biosens. Bioelectron.*, 112 (2018) 156.
12. K. Yan, Y. H. Yang, J. D. Zhang, *Sens. Actuators. B*, 259 (2018) 394.
13. Y. Y. Qi, J. H. He, F. R. Xiu, X. Yu, X. Gao, Y. F. Li, Y. W. Lu, Z. Q. Song, *Microchem. J.*, 147 (2019) 789.
14. Z. Q. Zhu, C. Jing, X. Y. Miao, Y. Shen, *Int. J. Electrochem. Sci.*, 15 (2020) 3969.
15. S. Su, Z. W. Lu, J. L, Q. Hao, W. Liu, C. C. Zhu, X. Z. Shen, J. Y. Shi and L. H. Wang, *New J. Chem.*, 42 (2018) 6750.
16. Y. Yun, *Int. J. Electrochem. Sci.*, 11 (2016) 2778.
17. Ş. U. Karabiberoglu, *Electroanalysis*, 31 (2019) 91.
18. N. B. Messaoud, M. E. Ghica, C. Dridi, M. B. Ali, C. M. Brett, *Sens. Actuators. B*, 253 (2017) 513.
19. N. Huang, M. L. Liu, H. T. Li, Y. Y. Zhang, S. Z. Yao, *Anal. Chim. Acta.*, 853 (2015) 249.
20. N. B. Messaoud, A. A. Lahcen, C. Dridi, A. Amine, *Sens. Actuators. B*, 276 (2018) 304.
21. F. Ianesko, C. A. Lima, C. Antoniazzi, E. R. Santana, J. V. Piovesan, A. Spinelli, A. Galli, E. G. Castro, *Electroanalysis*, 30 (2018) 1946.
22. U. Sidwaba, N. Ntshongontshi, U. Feleni, L. Wilson, T. Waryo, E. I. Iwuoha, *Electrocatalysis*, 10 (2019) 323.
23. D. Kim, J. Resasco, Y. Yu, A. M. Asiri, P. D. Yang, *Nat. Commun.*, 5 (2014) 1.
24. G. Sharma, A. Kumar, S. Sharma, M. Naushad, R. P. Dwivedi, Z. A. Alothman, G. T. Mola, *J. King. Saud. Univ. Sci.*, 31 (2017) 257.
25. X. Y. Li, X. Z. Du, *Sens. Actuators. B*, 239 (2017) 536.
26. V. Abdelsayed, A. Aljarash, M. S. Elshall, Z. A. Othman, A. H. Alghamdi, *Chem. Mater.*, 21 (2009) 2825.
27. X. Q. Huang, Y. J. Li, Y. J. Li, H. L. Zhou, X. F. Duan, Y. Huang, *Nano. Lett.*, 12 (2012) 4265.
28. K. N. Zhang, X. L. Chen, L. N. Wang, D. X Zhang, Z. H. Xue, X. B. Zhou, X. Q. Lu, *Int. J. Hydrogen Energy.*, 43 (2018) 15931.
29. X. Wang, Y. R. Shi, J. J. Shan, H. Zhou, M. J. Li, *Ionics*, 26 (2020) 3135.
30. E. Laviron, *J. Electroanal. Chem.*, 101 (1979) 19.
31. F. Pogacean, A. R. Biris, C. Socaci, M. Coros, L. Magerusan, M. Rosu, M. D. Lazar, G. Borodi, S. Pruneanu, *Nanotechnology*, 27 (2016) 484001.
32. T. Ndlovu, O. A. Arotiba, S. Sampath, R. W. Krause, B. B. Mamba BB, *Sensors*, 12 (2012) 11601.
33. M. Portaccio, D. D. Tuoro, F. Arduini, M. Lepore, D. G. Mita, N. Diano, L. Mita, D. Moscone D, *Biosens. Bioelectron.*, 25 (2010) 2003.
34. L. L. Zhu, Y. H. Cao, G. Q. Cao *Biosens. Bioelectron.*, 54 (2014) 258.
35. N. Teymoori, J. Raoof, M. A. Khalilzadeh, R. Ojani, *J. Iran. Chem. Soc.*, 15 (2018) 2271.